A TRANSPORT MATRIX ALGORITHM FOR THE STATIC ANALYSIS OF CIRCULAR HELICOIDAL BARS

S. A. Alghamdi*

Department of Civil Engineering
King Fahd University of Petroleum & Minerals
Dhahran, Saudi Arabia

الخلاصـــة :

يُـقـدِّم هذا البحث طريقة صـمُـمّت للقيام بالتحليل الإستاتيكي لقضبان حلزونية الدوران ، وقد صيغت معادلات التوازن الأستاتيكي والتشوهات لوصلة حلزونية بناءً على اشتقاق دوال النقل ، ومن ثم تستخدم هذه المعادلات لتحديد حالة الإجهاد والتشوه في أي مقطع على امتداد أي قضيب حلزوني . وإضافة إلى فائدتها في تحليل الحلزونيات المنفردة وتطويرها المنتظم - فإنّ الطريقة المقـدَّمـة تُـعتبر ذات فائدة متميزة لحساب التفاعل الهيكلي الناشيء بين القضبان الحلزونية وبين مجموعة أخرى من العناصر الإنشائية .

ABSTRACT

This paper presents a numerical procedure which has been devised to perform the static analysis of circular helicoidal bars. Based upon derived transfer functions, the equations of static equilibrium and deformations are formulated for a representative helicoid. These equations are then used to determine the state of stress and/or deformation at any section along the bar. In addition to its usefulness for the analysis of freely standing helicoids, and due to its systematic development, the method is particularly useful to account for the interaction between helicoidal bars and any other aggregate of structural members.

*Address for correspondence:
KFUPM Box No. 1896
King Fahd University of Petroleum & Minerals
Dhahran 31261
Saudi Arabia

A TRANSPORT MATRIX ALGORITHM FOR THE STATIC ANALYSIS OF CIRCULAR HELICOIDAL BARS

NOTATION

The following symbols are used:

a_o	opening angle for the bars
a	position angle of a point along the bar with respect to global coordinate system $x^o y^o z^o$
$\bar{a}$	opening angle of a helicoidal segment
a_1	opening angle of point p measured from left end of the segment
a_2	$\bar{a} - a_1$
A_i	ith transport function evaluated at $a = a_1$
A_x	area of cross section
B_i	ith transport function evaluated at $a = a_2$
$\bar{D}(a)$	state vector of deformations: u, v, w, ϕ, ψ, θ at angle a
E	modulus of elasticity
$\bar{F}_L^L$	scaled transport load vector at left end expressed in local system
$\bar{G}_R^R$	scaled transport load vector at right end expressed in local system
$\bar{H}(a)$	total vector of forces and deformations at angle a
I_{xx}; I_{yy}; I_{zz}	moments of inertia about the local x^l, y^l, z^l axes, respectively
k	number of terms used in the series solution of equation (2) below
l	superscript ^{l} to indicate local coordinate system
$\bar{L}(a)$	total transport load vector of forces and/or imposed deformations
$\bar{L}_1(a)$	transport load vector of applied forces
$\bar{M}$	matrix of constant coefficients
o	superscript ^{o} to indicate global coordinate system
$p_x(a)$; $p_y(a)$; $p_z(a)$	intensity of applied uniform forces
$P_x(a)$; $P_y(a)$; $P_z(a)$	applied singular forces
$q_x(a)$; $q_y(a)$; $q_z(a)$	intensity of applied uniform moments
$Q_x(a)$; $Q_y(a)$; $Q_z(a)$	applied singular moments
R	radius of the helical line
$\bar{S}(a)$	state vector of stress resultants: U, V, W, X, Y, Z at angle a
T_{LR}^{LR}	transport matrix (12×12)
$\bar{\alpha}$	helix angle
α	cos $\bar{\alpha}$
β	sin $\bar{\alpha}$
λ	cross section aspect ratio b/h
ξ_1	scale factor R/α

INTRODUCTION

Curvilinear space bars in the form of a circular helicoid (see Figure 1 for complete description of the geometry) have been in use since well before the turn of this century. Their aesthetic characteristics have been the primary reasons behind the use of these bars. Back then, technical knowledge on the structural analysis was still in its infancy and material technology was almost non-existent. Designers, consequently, relied mainly on intuition and common sense to proportion structures for specified loads. Under these circumstances, the use of sweeping

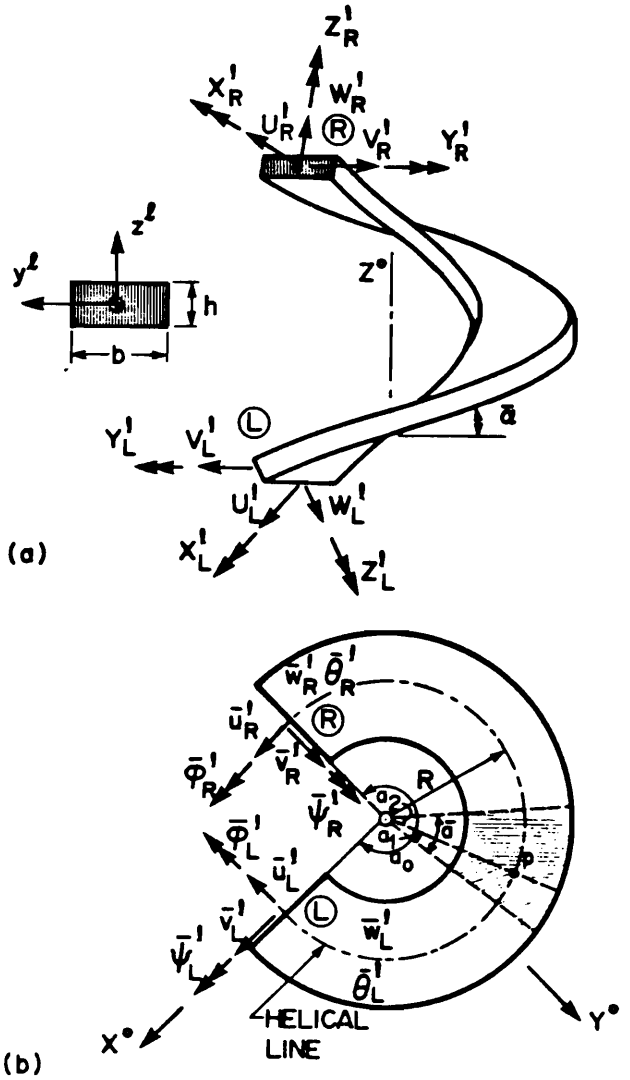

Figure 1. Helicoidal Element:
(a) Spatial Configuration in $X^oY^oZ^o$ System;
(b) Horizontal Projection in X^oY^o Plane.

assumptions have led to over-designs which [by our standards today] fall severely short of any measure of structural effectiveness.

With the availability of classical methods of structural analysis [namely: Flexibility (Force) and Stiffness (Displacement) Method] and with the development of the finite element method in the early 1960s, there has been a renewed interest in devising analytical and/or numerical procedures suitable for the analysis of circular helicoidal bars. To this end, several prominent researchers have made contributions towards a systematic analysis. The published contributions have, however, been limited to specialized cases of loadings and/or boundary conditions. The work of Holmes [1], for instance, is perhaps the first comprehensive study on the subject. Shortly afterwards, Scordelis [2] used the method of flexibilities to determine the stress resultants at specific points in the bar and to evaluate how the cross section aspect ratio ($\lambda = b/h$) affects the internal forces. The results are informative but limited in scope for the same reasons as indicated early. In addition to this, and by writing the strain energy expressions, Lee [3] used Castigliano's theorem to obtain the flexibility matrix. Because of the complex nature of the flexibility terms derived, this method can only be implemented to build the numerical form of the stiffness matrix. To the author's knowledge all known general purpose structural analysis programs do not — as yet — have the capability to account for the interaction of circular helicoidal bars with other structural members.

With the availability of powerful digital computers of different capacities and brands, even the most complicated form of structural configuration can nowadays be analyzed with relative ease. For helicoidal bars this task can be achieved once the governing differential equations are formulated. These equations have recently been formulated by the author [4]; but because of the high degree of coupling among the equations [5] the development of analytical solutions for them is beyond all practical means. Therefore the author has devised a transfer-matrix-based numerical method [6, 7] which can handle the problem of a bar with any combination of loads and plausible boundary conditions.

Within the framework of linear static analysis, this paper presents: (1) the transfer (transport) matrices; (2) the load effects vectors for a representative bar and typical loadings; (3) the implementation of the method on a digital computer is illustrated by a parametric study to determine practical ranges of the design variables which would make the bar functionally most efficient.

GOVERNING DIFFERENTIAL EQUATIONS

With reference to Figure 1(*b*), the geometry of typical segment of a circular helicoid is completely described by the helix angle $\bar{\alpha}$, the radius R of the centroidal line and the opening angle da. For this element the differential equations of equilibrium and deformations — within the framework of linear elasticity and neglecting shear deformations — can be written in dimensionless form as

$$\frac{d}{da}\begin{bmatrix}\bar{S}(a)\\ \bar{D}(a)\end{bmatrix} = \left[\begin{array}{c|c}\bar{M}_1 & O\\ \hline \bar{M}_2 & -\bar{M}_1^T\end{array}\right]\begin{bmatrix}\bar{S}(a)\\ \bar{D}(a)\end{bmatrix} + \begin{bmatrix}\bar{L}_1(a)\\ O\end{bmatrix}, \quad (1)$$

in which da is the angle subtended between ends of the segment; $\bar{S}(a)$ is a (6×1) vector of scaled internal forces and moments; $\bar{D}(a)$ is a (6×1) vector of scaled displacements and rotations; $\bar{L}_1(a)$ is a (6×1) vector of forces and moments representing the load on the segment.

To simplify the presentation, Equation (1) can be written in the following reduced symbolic form:

$$\frac{d}{da}\,\bar{H}(a) = \bar{M}\,\bar{H}(a) + \bar{L}(a)\,, \quad (2)$$

where the correspondence between Equation (1) and Equation (2) indicates that $\bar{H}(a)$ is a (12×1) vector comprising the stress resultants and deformations; $\bar{M}$ is a (12×12) matrix of constant coefficients representing geometry characteristics and material properties; and $\bar{L}(a)$ is a (12×1) vector which accounts for imposed forces and/or deformations.

And while a full account of the derivation of Equation (1) is given elsewhere [4], it suffices here to realize its dependence on:

(*a*) matrix $\bar{M}_1$ (6×6) which has the following form

$$\bar{M}_1 = \left[\begin{array}{ccc|ccc} 0 & \alpha & 0 & & & \\ -\alpha & 0 & \beta & & 0 & \\ 0 & -\beta & 0 & & & \\ \hline 0 & 0 & 0 & 0 & \alpha & 0 \\ 0 & 0 & \xi_1 & -\alpha & 0 & \beta \\ 0 & -\xi_1 & 0 & 0 & -\beta & 0 \end{array}\right], \quad (3)$$

where $\alpha = \cos\bar{\alpha}$; $\beta = \sin\bar{\alpha}$; $\xi_1 = R/\alpha$.

(*b*) matrix $\bar{M}_2$ (6,6) which has only the following non-zero elements

$$\bar{M}_2(1,1) = \xi_1/EA_x;\ \bar{M}_2(4,4) = \xi_1/EI_{xx}$$

$$\bar{M}_2(5,5) = \xi_1/EI_{yy};\ \bar{M}_2(6,6) = \xi_1/EI_{zz}. \quad (4)$$

(*c*) load vector $\bar{L}_1$ (6×1) which comprises the combined effect of all external causes:

$$\bar{L}_1(a) = [\xi_1^3 p_x(a);\ \xi_1^3 p_y(a);\ \xi_1^3 p_z(a);$$
$$\xi_1^2 q_x(a);\ \xi_1^2 q_y(a);\ \xi_1^2 q_z(a)]^T, \quad (5)$$

in which p's are distributed forces and q's are distributed moments along a differential segment of length $ds = R \sec\bar{\alpha}\ da$.

TRANSPORT FUNCTIONS

The spatial nature of helicoidal bars makes the process of relating stress resultants to their causes and evaluating deformations quite involved. The lengthy nature of the resulting expressions has made the implementation process a task imbued with massive amounts of numeric processing, to the extent that identification of basic modes deformation is practically obscured. This difficulty can be easily overcome by the use of transport functions.

The influence of loads and deformations imposed at a specific section of a bar is evaluated at another section by a set of functions containing all geometry and material characteristics. In principle, the exact form of the functions would naturally be a by-product of an analytical solution of Equation (2). However, since such a solution is beyond all practical means, a suitable alternative is to seek a numerical solution utilizing the transport matrix method. To this end, and using the Cayley–Hamilton theorem, the homogeneous solution of Equation (2) — without loading term — can be symbolically expressed as

$$\bar{H}(a_i) = \sum_{k=1}^{\infty} \left[\frac{\bar{M}^{k-1}}{(k-1)!} \cdot a^{k-1} \right] \bar{H}(a_{i-1}), \quad (6)$$

in which $\bar{H}(a_i)$, $\bar{H}(a_{i-1})$ are the state vectors at sections i and $i-1$, respectively.

By a very extensive and laborious algebraic manipulations, the matrix operations in Equation (6) has been evaluated and used to define a matrix T_{RL}^{RL} (12×12) such that

$$\bar{H}(a_i) = T_{RL}^{RL}\ \bar{H}(a_{i-1}) \quad (7)$$

in which R and L correspond to indices i and $i-1$, respectively.

To simplify the notation and discussions, Equation (7) is rewritten for a bar segment LR as

$$\bar{H}_R = T_{RL}^{RL}\ \bar{H}_L\ . \quad (8)$$

In this form the evaluation of load vector $\bar{L}(a)$ is easily explained by introducing two vectors $\bar{F}_L^L$ and $\bar{G}_R^R$ to represent load effects at L and R, respectively. Components of these two vectors have their physical meanings and can be thought of as the reactions and the transmitted displacement gap — by a rigid body motion — at the fixed end [7]. Consequently, for a segment under general type of loading and/or imposed deformations, Equation (8) can be written as:

$$\bar{H}_R = T_{RL}^{RL}\ \bar{H}_L + \bar{G}_R^R\ , \quad (9)$$

or — upon inverting — as:

$$\bar{H}_L = T_{LR}^{LR}\ \bar{H}_R + \bar{F}_L^L\ . \quad (10)$$

Equations (9) and (10) represent the basis of the method presented in this paper. These equations are presented in full in Tables 1 and 2. It should, however, be mentioned here that the successful implementation of the method relies heavily on the availability of load function vectors $\bar{F}_L^L$ and $\bar{G}_R^R$. In essence, the development of load functions for any type of loading should not be difficult. However, it has been done herein only for two particular types of loading. For a set of singular moments and uniform forces on portion of the bar the results are given in Tables 3 and 4 in terms of specific values of the transport functions given as:

$$A_i = T_i(a_1) \quad (11)$$

$$B_i = T_i(a_2) \quad (12)$$

$$C_i = T_i(a) - A_i\ . \quad (13)$$

where A_i — for example — is the transport function evaluated for bar segment with opening angle a_1, and can be thought of as a participation factor indicating how each external cause contribute to a specified stress resultant or mode of deformation.

APPLICATIONS

The method has been implemented in a computer program [named: HELIXS] written in the Fortran language and designed to run on AMDAHL 5850 mainframe computer with 16 MB of real storage. The PC version of the program is being developed but at present only the main frame version is available from the author. In its present form the program — and despite the general nature of the method — can be

Table 1. Static Transport Matrix Equations $\bar{H}_L^L = T_{LR}^{LR}\,\bar{H}_R^R + \bar{F}_R^R$

$$
\begin{bmatrix} \bar{U} \\ \bar{V} \\ \bar{W} \\ \bar{X} \\ \bar{Y} \\ \bar{Z} \\ \bar{u} \\ \bar{v} \\ \bar{w} \\ \bar{\phi} \\ \bar{\psi} \\ \bar{\theta} \end{bmatrix}_L
=
\left[\begin{array}{ccc|ccc|ccc|ccc}
T_1 & T_4 & T_7 & 0 & 0 & 0 & 0 & 0 & 0 & 0 & 0 & 0 \\
T_2 & T_5 & T_8 & 0 & 0 & 0 & 0 & 0 & 0 & 0 & 0 & 0 \\
T_3 & -T_6 & T_9 & 0 & 0 & 0 & 0 & 0 & 0 & 0 & 0 & 0 \\
\hline
T_{10} & T_{13} & T_{16} & T_{19} & T_{22} & T_{25} & 0 & 0 & 0 & 0 & 0 & 0 \\
T_{11} & T_{14} & T_{17} & T_{20} & T_{23} & T_{26} & 0 & 0 & 0 & 0 & 0 & 0 \\
T_{12} & T_{15} & T_{18} & T_{21} & T_{24} & T_{27} & 0 & 0 & 0 & 0 & 0 & 0 \\
\hline
-T_{28} & T_{29} & -T_{30} & -T_{34} & -T_{37} & -T_{40} & T_1 & -T_2 & T_3 & T_{10} & -T_{11} & T_{12} \\
-T_{29} & -T_{31} & T_{32} & -T_{35} & -T_{38} & -T_{41} & -T_4 & T_5 & -T_6 & -T_{13} & T_{14} & -T_{15} \\
-T_{30} & -T_{32} & -T_{33} & -T_{36} & -T_{39} & -T_{42} & T_7 & -T_8 & T_9 & T_{16} & -T_{17} & T_{18} \\
\hline
-T_{34} & T_{35} & -T_{36} & -T_{43} & T_{44} & -T_{45} & 0 & 0 & 0 & T_{19} & -T_{20} & T_{21} \\
T_{37} & -T_{38} & T_{39} & -T_{44} & -T_{46} & T_{47} & 0 & 0 & 0 & -T_{22} & T_{23} & -T_{24} \\
-T_{40} & T_{41} & -T_{42} & -T_{45} & -T_{47} & -T_{48} & 0 & 0 & 0 & T_{25} & -T_{26} & T_{27}
\end{array}\right]_{LR}
\begin{bmatrix} \bar{U} \\ \bar{V} \\ \bar{W} \\ \bar{X} \\ \bar{Y} \\ \bar{Z} \\ \bar{u} \\ \bar{v} \\ \bar{w} \\ \bar{\phi} \\ \bar{\psi} \\ \bar{\theta} \end{bmatrix}_R
+
\begin{bmatrix} \bar{F}_U \\ \bar{F}_V \\ \bar{F}_W \\ \bar{F}_X \\ \bar{F}_Y \\ \bar{F}_Z \\ \bar{F}_u \\ \bar{F}_v \\ \bar{F}_w \\ \bar{F}_\phi \\ \bar{F}_\psi \\ \bar{F}_\theta \end{bmatrix}_L
$$

Table 2. Static Transport Matrix Equations $\bar{H}_R^R = T_{RL}^{RL}\,\bar{H}_L^L + \bar{G}_R^R$

$$
\begin{bmatrix} \bar{U} \\ \bar{V} \\ \bar{W} \\ \bar{X} \\ \bar{Y} \\ \bar{Z} \\ \bar{u} \\ \bar{v} \\ \bar{w} \\ \bar{\phi} \\ \bar{\psi} \\ \bar{\theta} \end{bmatrix}_R
=
\left[\begin{array}{ccc|ccc|ccc|ccc}
T_1 & -T_4 & T_7 & 0 & 0 & 0 & 0 & 0 & 0 & 0 & 0 & 0 \\
-T_2 & T_5 & T_8 & 0 & 0 & 0 & 0 & 0 & 0 & 0 & 0 & 0 \\
T_3 & -T_6 & T_9 & 0 & 0 & 0 & 0 & 0 & 0 & 0 & 0 & 0 \\
\hline
T_{10} & -T_{13} & T_{16} & T_{19} & -T_{22} & T_{25} & 0 & 0 & 0 & 0 & 0 & 0 \\
T_{11} & T_{14} & -T_{17} & -T_{20} & T_{23} & -T_{26} & 0 & 0 & 0 & 0 & 0 & 0 \\
T_{12} & -T_{15} & T_{18} & T_{21} & -T_{24} & T_{27} & 0 & 0 & 0 & 0 & 0 & 0 \\
\hline
T_{28} & T_{29} & T_{30} & T_{34} & -T_{37} & T_{40} & T_1 & -T_2 & T_3 & T_{10} & -T_{11} & T_{12} \\
-T_{29} & T_{31} & T_{32} & -T_{35} & T_{38} & -T_{41} & -T_4 & T_5 & -T_6 & -T_{13} & T_{14} & -T_{15} \\
T_{30} & -T_{32} & T_{33} & T_{36} & -T_{39} & T_{42} & T_7 & -T_8 & T_9 & T_{16} & -T_{17} & T_{18} \\
\hline
T_{34} & T_{35} & T_{36} & T_{43} & T_{44} & T_{45} & 0 & 0 & 0 & T_{19} & T_{20} & T_{21} \\
T_{37} & T_{38} & T_{39} & -T_{44} & T_{46} & T_{47} & 0 & 0 & 0 & -T_{22} & T_{23} & T_{24} \\
T_{40} & T_{41} & T_{42} & T_{45} & -T_{47} & T_{48} & 0 & 0 & 0 & T_{25} & T_{26} & T_{27}
\end{array}\right]_{RL}
\begin{bmatrix} \bar{U} \\ \bar{V} \\ \bar{W} \\ \bar{X} \\ \bar{Y} \\ \bar{Z} \\ \bar{u} \\ \bar{v} \\ \bar{w} \\ \bar{\phi} \\ \bar{\psi} \\ \bar{\theta} \end{bmatrix}_L
+
\begin{bmatrix} \bar{G}_U \\ \bar{G}_V \\ \bar{G}_W \\ \bar{G}_X \\ \bar{G}_Y \\ \bar{G}_Z \\ \bar{G}_u \\ \bar{G}_v \\ \bar{G}_w \\ \bar{G}_\phi \\ \bar{G}_\psi \\ \bar{G}_\theta \end{bmatrix}_R
$$

used only for the analysis of prismatic helicoidal bar with any combination of boundary and load conditions. For the static analysis of a given bar, the input to the program includes data for: (1) definition of geometry; (2) type of cross section; (3) type, magnitude and location of loads; and (4) type of boundary conditions. The geometry is specified in terms of radius R and angles a and $\bar{\alpha}$. And with respect to the right-handed coordinate system given in Figure 1 the position coordinate of material points on the helicoidal surface are determined by the program. The program can handle any combination of singular, uniform, linear forces and moments acting anywhere along the helicoidal line. On the other

Table 3. Transport Load Functions: Concentrated Moments

$\bar{\alpha}$ = helix angle R = radius of helix $\xi_1 = R/\alpha$

For x, y, and z: $\bar{Q} = \xi_1 Q$

$\bar{F}_U = 0$	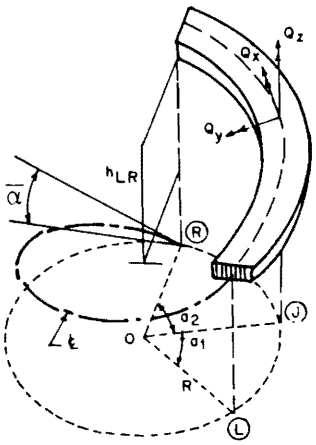	$\bar{G}_U = 0$
$\bar{F}_V = 0$		$\bar{G}_V = 0$
$\bar{F}_W = 0$		$\bar{G}_W = 0$
$\bar{F}_X = A_{19}\bar{Q}_x + A_{22}\bar{Q}_y + A_{25}\bar{Q}_z$		$\bar{G}_X = -B_{19}\bar{Q}_x + B_{22}\bar{Q}_y - B_{25}\bar{Q}_z$
$\bar{F}_Y = A_{20}\bar{Q}_x + A_{23}\bar{Q}_y + A_{26}\bar{Q}_z$		$\bar{G}_Y = B_{20}\bar{Q}_x - B_{23}\bar{Q}_y + B_{26}\bar{Q}_z$
$\bar{F}_Z = A_{21}\bar{Q}_x + A_{24}\bar{Q}_y + A_{27}\bar{Q}_z$		$\bar{G}_Z = -B_{21}\bar{Q}_x + B_{24}\bar{Q}_y - B_{27}\bar{Q}_z$
$\bar{F}_u = -A_{34}\bar{Q}_x - A_{37}\bar{Q}_y - A_{40}\bar{Q}_z$		$\bar{G}_u = -B_{34}\bar{Q}_x + B_{37}\bar{Q}_y - B_{40}\bar{Q}_z$
$\bar{F}_v = -A_{35}\bar{Q}_x - A_{38}\bar{Q}_y - A_{41}\bar{Q}_z$		$\bar{G}_v = B_{35}\bar{Q}_x - B_{38}\bar{Q}_y + B_{41}\bar{Q}_z$
$\bar{F}_w = -A_{36}\bar{Q}_x - A_{39}\bar{Q}_y - A_{42}\bar{Q}_z$		$\bar{G}_w = -B_{36}\bar{Q}_x + B_{39}\bar{Q}_y - B_{42}\bar{Q}_z$
$\bar{F}_\phi = -A_{43}\bar{Q}_x + A_{44}\bar{Q}_y - A_{45}\bar{Q}_z$		$\bar{G}_\phi = -B_{43}\bar{Q}_x - B_{44}\bar{Q}_y - B_{45}\bar{Q}_z$
$\bar{F}_\psi = -A_{44}\bar{Q}_x - A_{46}\bar{Q}_y + A_{47}\bar{Q}_z$		$\bar{G}_\psi = B_{44}\bar{Q}_x - B_{46}\bar{Q}_y - B_{47}\bar{Q}_z$
$\bar{F}_\theta = -A_{45}\bar{Q}_x - A_{47}\bar{Q}_y - A_{48}\bar{Q}_z$		$\bar{G}_\theta = -B_{45}\bar{Q}_x + B_{47}\bar{Q}_y - B_{48}\bar{Q}_z$

Table 4. Transport Load Functions: Partial Uniform Distributed Forces

$\bar{\alpha}$ = helix angle (rad) R = radius of helix For x, y, and z: $\bar{p} = \xi_1^3 p$

$\alpha = \cos\bar{\alpha}$ $\xi_1 = \dfrac{R}{\alpha}$

$\bar{F}_U = (C_1 + a_2)\bar{p}_x + C_4\bar{p}_y + C_7\bar{p}_z$	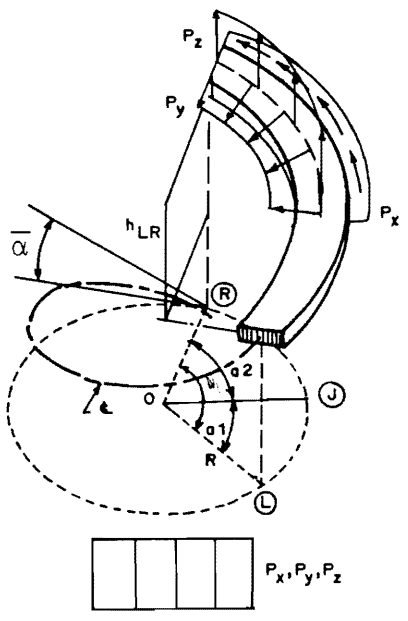	$\bar{G}_U = -((B_1 + a_2)\bar{p}_x - B_4\bar{p}_y + B_7\bar{p}_z)$
$\bar{F}_V = C_2\bar{p}_x + (C_5 + a_2)\bar{p}_y + C_8\bar{p}_z$		$\bar{G}_V = B_2\bar{p}_x - (B_5 + a_2)\bar{p}_y - B_8\bar{p}_z$
$\bar{F}_W = C_3\bar{p}_x - C_6\bar{p}_y + (C_9 + a_2)\bar{p}_z$		$\bar{G}_W = -(B_3\bar{p}_x - B_6\bar{p}_y + (B_9 + a_2)\bar{p}_z)$
$\bar{F}_X = C_{10}\bar{p}_x + C_{13}\bar{p}_y + C_{16}\bar{p}_z$		$\bar{G}_X = -(B_{10}\bar{p}_x - B_{13}\bar{p}_y + B_{16}\bar{p}_z)$
$\bar{F}_Y = C_{11}\bar{p}_x + C_{14}\bar{p}_y + C_{17}\bar{p}_z$		$\bar{G}_Y = B_{11}\bar{p}_x - B_{14}\bar{p}_y + B_{17}\bar{p}_z$
$\bar{F}_Z = C_{12}\bar{p}_x + C_{15}\bar{p}_y + C_{18}\bar{p}_z$		$\bar{G}_Z = -(B_{12}\bar{p}_x - B_{15}\bar{p}_y + B_{18}\bar{p}_z)$
$\bar{F}_u = -C_{28}\bar{p}_x + C_{29}\bar{p}_y - C_{30}\bar{p}_z$		$\bar{G}_u = -B_{28}\bar{p}_x - B_{29}\bar{p}_y - B_{30}\bar{p}_z$
$\bar{F}_v = -C_{29}\bar{p}_x - C_{31}\bar{p}_y + C_{32}\bar{p}_z$		$\bar{G}_v = B_{29}\bar{p}_x - B_{31}\bar{p}_y - B_{32}\bar{p}_z$
$\bar{F}_w = -C_{30}\bar{p}_x - C_{32}\bar{p}_y - C_{33}\bar{p}_z$		$\bar{G}_w = -B_{30}\bar{p}_x + B_{32}\bar{p}_y - B_{33}\bar{p}_z$
$\bar{F}_\phi = -C_{34}\bar{p}_x + C_{35}\bar{p}_y - C_{36}\bar{p}_z$		$\bar{G}_\phi = -B_{34}\bar{p}_x - B_{35}\bar{p}_y - B_{36}\bar{p}_z$
$\bar{F}_\psi = C_{37}\bar{p}_x - C_{38}\bar{p}_y + C_{39}\bar{p}_z$		$\bar{G}_\psi = -B_{37}\bar{p}_x - B_{38}\bar{p}_y - B_{39}\bar{p}_z$
$\bar{F}_\theta = -C_{40}\bar{p}_x + C_{41}\bar{p}_y - C_{42}\bar{p}_z$		$\bar{G}_\theta = -B_{40}\bar{p}_x - B_{41}\bar{p}_y - B_{42}\bar{p}_z$

hand, the output includes: (1) a summary of input data; (2) a listing of stress resultants and deformations at selected points; and (3) a summary of the maximum values of internal forces and deformations.

To demonstrate application of the method, the results of two example problems are presented. In the first problem a parametric study is performed to assess how the cross section aspect ratio λ affect the magnitude of maximum values of internal forces and deformations. For a steel bar [$E = 4.32 \times 10^7$ ksf; $\nu = 0.3$; $a_0 = 360°$] with only 10 kips singular forces in the negative $z°$-direction [at $a = 90°$; 180°; and 270°], a summary of maximum internal forces and deformations is given in Table 5.

The second example presents the analysis of a steel bar loaded by a combination of singular forces P_x, P_y, P_z and singular moments Q_x, Q_y, Q_z at selected position angles along the helicoidal line. A complete catalog of input and output results is given in Table 6.

DISCUSSIONS AND CONCLUDING REMARKS

To some extent the development of an analytical model which can be used for the static analysis of helicoidal bars is — at present — beyond all practical means and would be, at least a time consuming process. This has led the author to develop an automated numerical procedure by which the static analysis of such bars is reduced to a routine process.

On the basis of a derived transport matrix T_{RL}^{RL} (which combines the state vectors $\bar{H}_L^L$, $\bar{H}_R^R$ to load vectors $\bar{F}_L^L$ and $\bar{G}_R^R$) the computer code HELIXS has been developed to perform the analysis on main-frame computer installations. For a prismatic bar, the input to the program requires only four parameters to describe the overall geometry; namely: (1) opening angle a; (2) helix angle $\bar{\alpha}$; (3) cross-section aspect ratio λ; and (4) radius of the helicoidal line. And compared to existing Finite Element programs — which are almost always known to require a laborious process of mesh generation — the program HELIXS may be considered superior at least on practical grounds.

In its present form, the program can be used — on a trial basis — to select an optimal preliminary design of geometrical configuration of a bar under specified loads. The result of a typical study — to this effect — as given in Table 5 indicates best performance of the bar when λ is selected between 2 and 10. On the other hand, the method and the program can be easily extended to develop the stiffness matrix and the stiffness load functions. The program can then be incorporated in a general Finite Element code to perform the structural analysis of structures involving helicoidal bars.

ACKNOWLEDGEMENTS

The numerical results reported in this paper have been performed on the main-frame computers of King Fahd University of Petroleum & Minerals, Dhahran, Saudi Arabia.

Table 5. Effect of λ on Maximum Values of Internal Forces and Displacement in a Circular Helicoidal Bar*

λ	0.5	1	4	8	10	16
U	12.9	14.2	15.6	15.7	15.8	15.8
V	6.24	7.57	9.36	9.53	9.55	9.57
W	21.6	21.6	21.6	21.6	21.6	21.6
X	−76.0	−54.7	−26.4	−23.7	−23.4	−23.0
Y	137.0	113.0	88.1	86.1	85.9	85.6
Z	−60.6	−86.2	−112.0	−115.0	−115.0	−115.0
u	-0.959×10^{-1}	0.117×10^{-1}	-0.315×10^{-2}	-0.162×10^{-2}	-0.130×10^{-2}	-0.814×10^{-3}
v	-0.598×10^{-1}	-0.521×10^{-2}	-0.189×10^{-2}	-0.973×10^{-3}	-0.781×10^{-3}	-0.490×10^{-3}
w	−0.438	-0.640×10^{-2}	-0.238×10^{-2}	-0.120×10^{-2}	-0.937×10^{-3}	-0.570×10^{-3}
ϕ	0.299×10^{-1}	0.401×10^{-2}	0.211×10^{-3}	0.963×10^{-4}	0.762×10^{-4}	0.470×10^{-4}
ψ	0.171×10^{-1}	-0.274×10^{-2}	-0.230×10^{-4}	-0.109×10^{-4}	-0.109×10^{-4}	-0.820×10^{-5}
θ	0.199×10^{-1}	0.302×10^{-2}	-0.890×10^{-4}	-0.560×10^{-4}	-0.460×10^{-4}	-0.290×10^{-4}

* Fixed−Fixed end conditions: $h = 1$ ft $R = 10$ ft $\bar{\alpha} = 30°$

Table 6. Input and Output for the Second Example Problem.

A: Input

Type of Structure : Steel Circular Helicoidal Ramp: $E = 210\,\text{GPa}$; $v = 0.30$

Geometry :

h	λ	R	a_0	$\bar{\alpha}$
0.5	10	20	360	30°

Boundary Condition : Fixed−Fixed

Loads	Magnitude	Position Angle (a)	
		Loads	Intermediate Supports
$P_x(a)$	−100 kN	at 90°, 180°, 270°	None
$P_y(a)$	−100 kN		
$P_z(a)$	−300 kN		
$Q_x(a)$	−50 kN		
$Q_y(a)$	−50 kN		
$Q_z(a)$	−100 kN		

B: Output*

Angle	Forces (Displacement)			Moments (Rotations)		
	U; (u)	V; (v)	W; (w)	X; (ϕ)	Y; (ψ)	Z; (θ)
$a = 0°$	98.91	−178.7	−398.3	−1635.3	−4628.0	6694.4
	(0.0)	(0.0)	(0.0)	(0.0)	(0.0)	(0.0)
$a = 360°$	498.8	221.4	801.7	−3516.6	1520.1	−904.3
	(0.0)	(0.0)	(0.0)	(0.0)	(0.0)	(0.0)
Max.	596.0	−499.0	584.0	864.0	3520.0	8110.0
Values	(-0.478×10^{-1})	(-0.326×10^{-1})	(-0.416×10^{-1})	(-0.160×20^{-2})	(-0.636×10^{-3})	(-0.799×10^{-3})

*All values are with respect to the local coordinate system $x^l\ y^l\ z^l$ and units are kN; m; rad.

REFERENCES

[1] A. M. C. Holmes, "Analysis of Helicoidal Beams Under Symmetrical Loading", *Proc. ASCE,* **83(6)** (1957), p. 1437-1.

[2] A. C. Scordelis, "Internal Forces in Uniformly Loaded Helicoidal Girders", *J. ACI,* **31(10)** (1960), p. 1013.

[3] H. P. Lee, "Generalized Stiffness Matrix of a Curved-Beam Elements", *AIAA Journal,* **7(10)** (1969), p. 2042.

[4] S. A. Alghamdi, *et. al.*, "Static Analysis of Helicoidal Bars", *Proc. 4th Int. Conf. Civil and Struct. Engrg. Computing, Civil-Comp. 89,* 1989, p. 247.

[5] P. S. Theocaris, *et. al.*, "A Theorem on the Decoupling of Higher Order Linear Differential Systems with Variable Coefficients", *Industrial Math.,* **33** (1983), p. 33.

[6] R. K. Livesley, *Matrix Methods of Structural Analysis,* 2nd edn. Oxford: Pergamon Press, 1975.

[7] J. J. Tuma, *Space Structural Analysis, Schaum's Series.* New York: McGraw−Hill, 1982.

Paper Received 9 January 1991; Revised 17 August 1991.